6-2004

Comparison of Discrete Singular Convolution and Generalised Differential Quadrature for the Vibration Analysis of Rectangular Plates

C. H. W. NG
National University of Singapore

Yibao ZHAO
Singapore Management University, ybzhao@smu.edu.sg

G. W. WEI
Michigan State University
DOI: https://doi.org/10.1016/j.cma.2004.01.013

Follow this and additional works at: https://ink.library.smu.edu.sg/lkcsb_research

Part of the Physical Sciences and Mathematics Commons

Citation

NG, C. H. W.; ZHAO, Yibao; and WEI, G. W.. Comparison of Discrete Singular Convolution and Generalised Differential Quadrature for the Vibration Analysis of Rectangular Plates. (2004). *Computer Methods in Applied Mechanics and Engineering*. 193, (23-26), 2483-2506. Research Collection Lee Kong Chian School Of Business.
Available at: https://ink.library.smu.edu.sg/lkcsb_research/927

Comparison of discrete singular convolution and generalized differential quadrature for the vibration analysis of rectangular plates

C.H.W. Ng [a], Y.B. Zhao [a], G.W. Wei [b,c,*]

[a] *Department of Computational Science, National University of Singapore, Singapore 117543, Singapore*
[b] *Department of Mathematics, Michigan State University, East Lansing, MI 48824, USA*
[c] *Department of Electrical and Computer Engineering, Michigan State University, East Lansing, MI 48824, USA*

Abstract

This paper presents a comprehensive comparison study between the discrete singular convolution (DSC) and the well-known global method of generalized differential quadrature (GDQ) for vibration analysis so as to enhance the understanding of the DSC algorithm. The DSC method is implemented through Lagrange's delta sequence kernel (DSC-LK), which utilizes local Lagrange polynomials to calculate weighting coefficients, whereas, the GDQ requires global ones. Moreover, it is shown that the treatments of boundary conditions and the use of grid systems are different in the two methods. Comparison study is carried out on 21 rectangular plates of different combinations of simply supported (S), clamped (C) and transversely supported with nonuniform elastic rotational restraint (E) edges, and five rectangular plates of mixed supporting edges, some of which with a range of aspect ratios and rotational spring coefficients. All the results of the DSC-LK agree very well with both those in the literature and newly computed GDQ results. Furthermore, it is observed that the DSC-LK performs much better for plates vibrating at higher-order eigenfrequencies. Unlike the GDQ, the DSC-LK is numerically stable for problems which require a large number of grid points.

Keywords: Discrete singular convolution; Generalized differential quadrature; Vibration analysis; Rectangular plates; Non-uniform boundary condition; Mixed boundary condition

1. Introduction

Plates are fundamental components in structural engineering. They are also proved to be useful models for more complex structural behavior. Apart from a few analytically solvable cases [1–3], there is no general solution for the vibration analysis of plates. Therefore, a large number of useful methods have been

---

[*] Corresponding author. Address: Department of Mathematics, Michigan State University, East Lansing, MI 48824, USA. Tel.:+1-517-353-4689.
E-mail address: wei@math.msu.edu (G.W. Wei).

developed to obtain solutions for many practical problems [5–19], when analytical methods fail or become too cumbersome. Typical successful numerical methods include the spline finite strip method by Fan and Cheung [4], the Galerkin approach by Chia [5] and Leipholz [6], the least squares technique [7] and meshless methods [8,9]. In particular, Rayleigh-Ritz methods [20–27], which have many successful applications in plate vibration analysis, utilize a set of global basis functions to approximate vibration eigenmodes. Finite element methods [28–31] often divide the domain of interest into a number of smaller sub-domains, and approximate the solution by using local, piecewise continuous shape functions. Differential quadrature (DQ) methods [32–36] have many successful applications in the vibration analysis. The DQ method was proposed by Bellman and coworkers in 1972 [32] and then virtually ignored until Bert and coworkers [33,34] brought in back to life in late 1980s. Since then, it has been recognized as a powerful approach in many science and engineering fields. The method is based on the idea that the partial derivative of a function with respect to a spatial variable at a given discrete point can be expressed as a weighted linear sum of the function values at all the discrete points in the computational domain. Shu and Richards [37] introduced the generalized differential quadrature (GDQ) [38–40] to simplify the calculation of the weighting coefficients. Some of the successful applications of the GDQ include plates with free edge supports [39] and mixed boundary conditions [40].

Recently, the discrete singular convolution (DSC) algorithm has been proposed for the computer realization of singular convolutions [41–43]. The underlying mathematical structure of the DSC algorithm is the theory of distributions [44] and wavelet analysis. The DSC algorithm can be regarded as a local spectral method. It exhibits global methods' accuracy and local methods' flexibility for handling complex geometry and boundary conditions in many applications. These successful applications include fluid dynamical simulation [45,46], nonlinear dynamics [47], pattern formation [48], shock capturing [49], and image processing [50]. What is the most relevant to the present work is the use of the DSC for structural analysis, including the vibration and buckling of beams [51], plate vibration under various edges and internal supports [45,52–55]. In particular, the vibration analyses of plates with irregular internal supports [55] and vibrating at higher-order modes [56,57] are very challenging tasks.

The objective of the present work is to explore the utility and to demonstrate the performance of the DSC algorithm for vibration analysis of plates through comprehensive comparison studies between the DSC and GDQ algorithms. The DSC algorithm is implemented by using the (unregularized) Lagrange's delta kernel (DSC-LK), which has not been accounted previously. Since both the DSC-LK and GDQ utilize Lagrange's kernels, it is expected that the present study provides an insight into both approaches. For completeness, it is worth mentioning that the Lagrange delta kernel is just one of many kernels available to the DSC algorithm [41–43]. This paper is organized as follows. Section 2 is devoted to the plate vibration formulation, the GDQ method and the DSC-LK formalism. The numerical results of GDQ and DSC-LK are presented and discussed in Section 3. Finally, a conclusion is given in Section 4.

2. Theory and algorithm

For integrity and completeness, this section accounts for the theory of plate analysis and methods of solution. However, the readers are highly recommended to refer to original works [37–41] for details of both methods. Particular emphasis is just given to a comparison study between the DSC-LK and GDQ algorithms so as to shed light on both methods.

2.1. Plate vibration

For a rectangular Kirchhoff plate (see Fig. 1) of length *a* and width *b*, the governing equation of free vibration is [3]
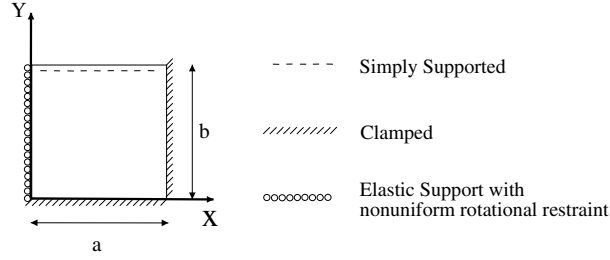
Fig. 1. Geometry and coordinate system of rectangular plate.

$$\frac{\partial^4 w}{\partial X^4} + 2\frac{\partial^4 w}{\partial X^2 \partial Y^2} + \frac{\partial^4 w}{\partial Y^4} = \frac{\rho h \omega^2}{D} w, \tag{1}$$

where w is the transverse displacement of the plate, X and Y are the Cartesian coordinates in the plane of the middle surface of the plate, ρ is the mass density per unit volume of the plate, D is the flexural rigidity of the plate ($D = Eh^3/[12(1-v^2)]$), E is Young's modulus of elasticity, h is the thickness of the plate, v is Poisson's ratio, and ω is the natural frequency of the plate. For generality, dimensionless governing equation is used,

$$\frac{\partial^4 W}{\partial x^4} + 2\lambda^2 \frac{\partial^4 W}{\partial x^2 \partial y^2} + \lambda^4 \frac{\partial^4 W}{\partial y^4} = \Omega^2 W, \tag{2}$$

where W is the dimensionless displacement ($W = w/a$), Ω is the dimensionless frequency parameter ($\Omega = \omega a^2 (\rho h/D)^{1/2}$), λ is the aspect ratio of the plate ($\lambda = a/b$), x and y are the dimensionless coordinates along the X- and Y-directions respectively ($x = X/a, y = Y/b$).

In this paper, three types of boundary conditions are considered in terms of the dimensionless parameters and coordinates, i.e.,

- Simply-supported edge (S)

$$W = 0, \quad -D\left(\frac{\partial^2 W}{\partial n^2} + v\frac{\partial^2 W}{\partial s^2}\right) = 0. \tag{3}$$

- Clamped edge (C)

$$W = 0, \quad \frac{\partial W}{\partial n} = 0. \tag{4}$$

- Transversely supported edge with non uniform elastic rotational restraint (E)

$$W = 0, \quad -D\left(\frac{\partial^2 W}{\partial n^2} + v\frac{\partial^2 W}{\partial s^2}\right) = K(s)\frac{\partial W}{\partial n}. \tag{5}$$

Here n and s are the normal and tangential directions of the plate respectively, $K(s)$ is the varying edge rotational spring coefficient. In this paper, the varying rotational spring coefficients on E edges are given separately, i.e., on the $x = 0$ and $x = 1$ edges,

$$K(y) = K'y(1-y), \tag{6}$$

and on the edges $y = 0$ and $y = 1$,

$$K(x) = K'x(1-x)/\lambda, \tag{7}$$

where K' is the dimensionless spring coefficient.

It is worth mentioning that free edge support is another important boundary condition. For the GDQ, free edge support can be implemented by directly coupling the boundary conditions with the governing equations, a technique referred to as CBCGE [39]. For the DSC, the present scheme proposed for handling boundaries is not suitable for the free boundary condition. This is because it requires boundary conditions with only partial derivatives normal to the edge. Free boundary condition involves mixed partial derivative and its directly implementation will degrade the DSC to the second order in accuracy. Certainly, one can adopt an algorithm similar to the CBCGE near the boundaries in the DSC. However, such a treatment will diminish the difference between the GDQ and DSC. Hence, further effort is required to make the DSC available for the free boundary condition.

2.2. Generalized differential quadrature

The general differential quadrature (GDQ) formulation can be found in some existing literature [37–40]. For integrity and convenience, this subsection reviews the main idea of the GDQ method rather than to reproduce the existing formulation. To approximate the derivative of a function with respect to a space variable at a given discrete point, the GDQ employs a weighted linear combination of the function values at all the discrete points in the direction of the space variable within the computational domain. For example, the mth derivative of a function $u(x)$ at the ith point, x_i, is approximated as

$$u^{(m)}(x_i) = \sum_{j=1}^{N} c_{i,j}^{(m)} u(x_j), \quad i = 1, 2, \ldots, N, \tag{8}$$

where $u_x^{(m)}(x_i)$ is the mth order derivative of $u(x)$ at x_i, N is the *total* number of grid points in the computational domain, $c_{i,j}^{(m)}$, $(j = 1, \ldots, N)$, are the weighting coefficients for the mth derivative approximation of the ith point. These coefficients have to be pre-determined.

In the GDQ method, the global Lagrange interpolation polynomial is used:

$$g_j(x) = \prod_{k=1, k \neq j}^{N} \frac{x - x_k}{x_j - x_k}, \quad j = 1, 2, \ldots, N. \tag{9}$$

In the existing GDQ literature, Eq. (9) is usually written in the form

$$g_j(x) = \frac{M(x)}{(x - x_j) M^{(1)}(x_j)}, \quad j = 1, 2, \ldots, N, \tag{10}$$

where

$$M(x) = \prod_{k=1}^{N} (x - x_k), \tag{11}$$

$$M^{(1)}(x_j) = \prod_{k=1, k \neq j}^{N} (x_j - x_k), \tag{12}$$

where $M^{(1)}(x)$ is the first derivative of $M(x)$. Thus, the weighting coefficients $c_{i,j}^{(1)}$ $(i, j = 1, 2, \ldots, N)$ can be obtained analytically from the differentiation of Eq. (10), i.e.,

$$c_{i,j}^{(1)} = g_j^{(1)}(x_i) \quad \text{for } i, j = 1, 2, \ldots, N, \ j \neq i, \tag{13}$$

and as for $i = j$,

$$c_{i,i}^{(1)} = - \sum_{j=1, j \neq i}^{N} c_{i,j}^{(1)} \quad \text{for } i = 1, 2, \ldots, N. \tag{14}$$

The weighting coefficients for higher order derivatives can be obtained through the following recurrence relationship [37]:

$$c_{i,j}^{(n)} = n\left(c_{i,j}^{(1)}c_{i,i}^{(n-1)} - \frac{c_{i,j}^{(n-1)}}{x_i - x_j}\right) \tag{15}$$

for $i, j = 1, 2, \ldots, N$, $j \neq i$ and $n = 2, 3, \ldots, N - 1$, and

$$c_{i,i}^{(n)} = -\sum_{j=1, j\neq i}^{N} c_{i,j}^{(n)} \tag{16}$$

for $i = 1, 2, \ldots, N$, $n = 2, 3, \ldots, N - 1$.

Let N be the number of grid points in both the x and y-directions. The GDQ approximation can be applied to Eq. (2) at each discrete point on the grid and the discretized governing equation at (x_i, y_j) is given by

$$\sum_{k=1}^{N} c_{i,k}^{(4)} W_{k,j} + 2\lambda^2 \sum_{k1=1}^{N} \sum_{k2=1}^{N} c_{i,k1}^{(2)} c_{j,k2}^{(2)} W_{k1,k2} + \lambda^4 \sum_{k=1}^{N} c_{j,k}^{(4)} W_{i,k} = \Omega^2 W_{i,j}, \ \ i, j = 1, 2, \ldots, N. \tag{17}$$

After the implementation the boundary conditions by substituting all the boundary conditions into the discretized governing equations, a technique referred to as SBCGE [37–40], Eq. (17) can be expressed as an eigenvalue and eigenvector problem

$$[A][W] = \Omega^2[W], \tag{18}$$

where

$$[W] = [W_{3,3}, \ldots, W_{3,N-2}, W_{4,3}, \ldots, W_{N-2,N-2}]^{\mathrm{T}}, \tag{19}$$

and $[A]$ is a $(N-4)^2 \times (N-4)^2$ matrix.

2.3. Discrete singular convolution

In this work, the DSC uses a formula similar to (8). To approximate the derivative of a function with respect to a space variable at a given discrete point, the DSC usually uses a weighted linear combination of the function values at $2M + 1$ points (M points to the left and M points to the right) in the direction of the space variable, where M is known as the half bandwidth. The mth derivative of a function $f(x)$ at the ith point, x_i, is then approximated as

$$f^{(m)}(x_i) \approx \sum_{j=-M}^{M} c_{i,j}^{(m)} f(x_{i+j}), \quad i = 0, 1, \ldots, N - 1. \tag{20}$$

Note that in Eq. (20), the summation indices differ from those of Eq. (8). Here $c_{i,j}^{(m)}$ can be calculated through DSC kernels. Many different kernels are used in our previous work [52]. In this paper, we utilize the nonregularized Lagrange's delta sequence kernel. Having a formula similar to (9), the DSC-LK considers, for $i = 0, \ldots, N - 1$ and $j = -M, \ldots, M$,

$$g_{i,j}(x) = \begin{cases} \prod_{k=i-M, k\neq i+j}^{i+M} \dfrac{x - x_k}{x_{i+j} - x_k}, & x_{i-M} \leqslant x \leqslant x_{i+M}, \\ 0, & \text{otherwise}. \end{cases} \tag{21}$$

Hence, the weighting coefficients for the first derivative can be obtained as follows:

$$c_{i,j}^{(1)} = g_{i,j}^{(1)}(x_i), \tag{22}$$

for $i = 0, 1, \ldots, N-1$, $j = -M, \ldots, M$, $j \neq 0$, and as   for $j = 0$,

$$c_{i,0}^{(1)} = -\sum_{j=-M, j \neq 0}^{M} c_{i,j}^{(1)} \quad \text{for } i = 0, 1, \ldots, N-1. \tag{23}$$

The weighting coefficients for higher order derivatives can be obtained using a recurrence formula similar to (15):

$$c_{i,j}^{(n)} = n\left(c_{i,j}^{(1)} c_{i,i}^{(n-1)} - \frac{c_{i,j}^{(n-1)}}{x_i - x_{i+j}} \right) \tag{24}$$

for $i = 0, 1, \ldots, N-1$, $j = -M, \ldots, M$, $j \neq 0$ and $n = 2, 3, \ldots, 2M$, and

$$c_{i,0}^{(n)} = -\sum_{j=-M, j \neq 0}^{M} c_{i,j}^{(n)} \tag{25}$$

for $i = 0, 1, \ldots, N-1$, $n = 2, 3, \ldots, 2M$.

For a uniform grid of N grid points for the computational domain, $x_0 < \cdots < x_{N-1}$, with a total of $2M$ fictitious grid points (ghost points), $x_{-M} < \cdots < x_{-1}$ and $x_N < \cdots < x_{N-1+M}$, i.e.,

$$x_i = x_0 + i\Delta x, \quad i = -M, \ldots, N-1+M. \tag{26}$$

From (13), (15), (22) and (24), it is observed that the values of $c_{i,j}^{(1)}$ and $c_{i,j}^{(n)}$ only depend on the index j. Hence $c_{i,j}^{(n)}$ can be converted into a single index as

$$C_j^{(n)} = c_{i,j}^{(n)}, \quad j = -M, \ldots, M, \quad \forall i \in \{0, 1, \ldots, N-1\}, \tag{27}$$

which gives a common set of $2M+1$ coefficients $\{C_{-M}^{(n)}, \ldots, C_M^{(n)}\}$ for every point in the computational domain, $x_0, \ldots, x_{N-1}$. Eq. (20) can be rewritten as

$$f^{(m)}(x_i) \approx \sum_{k=-M}^{M} C_k^{(m)} f(x_{i+k}) \quad \text{for } i = 0, 1, \ldots, N-1. \tag{28}$$

For simplicity, this paper only concerns the DSC-LK implemented on the uniform grid.

Numerically to solve the plate vibration governing equation, Eq. (2), it is necessary to give a matrix representation to the differential operator so that the action of the operator can be realized. From Eq. (28), we first define a differential matrix, $D_q^{(m)}$, by

$$[D_q^{(m)}]_{i,j} = \begin{cases} C_{j-i}^{(m)}, & \text{if } -M < j-i < M, \\ 0, & \text{otherwise}, \end{cases} \tag{29}$$

for $i = 0, \ldots, N-1$, $j = -M, \ldots, N-1+M$. Here $D_q^{(m)}$ is an $N \times (2M+N)$ differential matrix, q is the direction of differentiation ($q = x, y$) and m is the order of differentiation.

A complete numerical algorithm has to provide a scheme for handling boundaries. The Dirichlet boundary condition ($W = 0$) can be easily specified at the boundary. The implementation of the second boundary condition is illustrated by the one dimensional function, $f(x)$. An assumption on the relation between the ghost points and interior points on the left boundary (x_0 is the left boundary point) is given by

$$f(x_{-i}) - f(x_0) = a_i[(f(x_i) - f(x_0)], \quad \text{for } i = 1, \ldots, M, \tag{30}$$

where parameters $a_i, (i = 1, \ldots, M)$, are to be determined. After rearrangement, Eq. (30) becomes

$$f(x_{-i}) = a_i f(x_i) + (1 - a_i) f(x_0). \tag{31}$$

According to Eq. (28), the first and second derivative are approximated as

$$f'(x_0) = \sum_{i=-M}^{M} C_i^1 f(x_i) = \left[C_0^1 - \sum_{i=1}^{M} (1 - a_i) C_i^1 \right] f(x_0) + \sum_{i=1}^{M} (1 - a_i) C_i^1 f(x_i), \tag{32}$$

$$f''(x_0) = \sum_{i=-M}^{M} C_i^2 f(x_i) = \left[C_0^2 + \sum_{i=1}^{M} (1 - a_i) C_i^2 \right] f(x_0) + \sum_{i=1}^{M} (1 + a_i) C_i^2 f(x_i). \tag{33}$$

For simply supported edges, it is demonstrated that the boundary conditions are equivalent to

$$f(x_0) = 0, \quad f''(x_0) = 0. \tag{34}$$

These are satisfied by choosing $a_i = -1$, $i = 1, 2, \ldots, M$. This is called anti-symmetric extension.
   Similarly, for clamped edges, the boundary conditions

$$f(x_0) = 0, \quad f'(x_0) = 0 \tag{35}$$

are satisfied by choosing $a_i = 1$, $i = 1, 2, \ldots, M$. This is called symmetric extension.
   For transversely supported edges with non-uniform elastic rotational restraint, the boundary conditions
reduce to

$$f(x_0) = 0, \quad f''(x_0) - K f'(x_0) = 0. \tag{36}$$

Hence, the second boundary condition gives

$$\sum_{i=1}^{M} (1 + a_i) C_i^2 f(x_i) - K \sum_{i=1}^{M} (1 - a_i) C_i^1 f(x_i) = 0. \tag{37}$$

Further simplification of the above equation gives

$$\sum_{i=1}^{M} \left[(1 + a_i) C_i^2 - K(1 - a_i) C_i^1 \right] f(x_i) = 0. \tag{38}$$

One way to satisfy Eq. (38) is to choose

$$a_i = \frac{K C_i^1 - C_i^2}{K C_i^1 + C_i^2}, \quad i = 1, \ldots, M. \tag{39}$$

Expressions for the right boundary (at x_{N-1}) can be derived in a similar manner. Based on a corresponding
assumption that

$$f(x_{N-1+i}) - f(x_{N-1}) = a_i [f(x_{N-1-i}) - f(x_{N-1})], \quad \text{for } i = 1, \ldots, M, \tag{40}$$

we have

- Simply-supported edge

$$a_i = -1 \quad \text{for } i = 1, \ldots, M. \tag{41}$$

- Clamped edge

$$a_i = 1 \quad \text{for } i = 1, \ldots, M. \tag{42}$$

- Transversely supported edges with non uniform elastic rotation restraint edge (E)

$$a_i = \frac{KC_i^1 - C_i^2}{KC_i^1 + C_i^2} \quad \text{for } i = 1, \dots, M. \tag{43}$$

These are the same as those for the left boundary because the DSC weights depend only on the relative positions among the $2M + 1$ grid points. With appropriate choice of a_i (as computed above), weight coefficient for every ghost point outside the computational domain in the differential matrix, $D_q^{(m)}$, can be expressed as a weight coefficient for an interior point with corresponding scale factors. Hence, a new

Table 1
Convergence study: an SSSS plate ($\lambda = 1$)
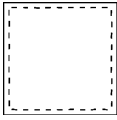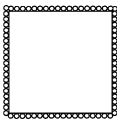
Plate	Method	Ω	$N = 16$	$N = 18$	$N = 20$	$N = 22$	$N = 24$
	DSC-LK with	1	19.739	19.739	19.739	19.739	19.739
	$M = 14$	2	49.348	49.348	49.348	49.348	49.348
		3	49.348	49.348	49.348	49.348	49.348
		4	78.957	78.957	78.957	78.957	78.957
		5	98.696	98.696	98.696	98.696	98.696
	DSC-LK with	1	19.739	19.739	19.739	19.739	19.739
	$M = N - 1$	2	49.348	49.348	49.348	49.348	49.348
		3	49.348	49.348	49.348	49.348	49.348
		4	78.957	78.957	78.957	78.957	78.957
		5	98.696	98.696	98.696	98.696	98.696
	GDQ	1	19.739	19.739	19.739	19.739	19.739
		2	49.348	49.348	49.348	49.348	49.348
		3	49.348	49.348	49.348	49.348	49.348
		4	78.957	78.957	78.957	78.957	78.957
		5	98.695	98.696	98.696	98.696	98.696

Table 2
Convergence study: an EEEE plate ($K' = 10$, $\lambda = 1$)

Plate	Method	Ω	$N = 16$	$N = 18$	$N = 20$	$N = 22$	$N = 24$
	DSC-LK with	1	23.188	23.175	23.165	23.158	23.152
	$M = 14$	2	53.066	53.034	53.011	52.994	52.981
		3	53.066	53.034	53.011	52.994	52.981
		4	82.367	82.322	82.290	82.266	82.249
		5	102.410	102.349	102.307	102.276	102.253
	DSC-LK with	1	23.188	23.175	23.165	23.158	23.152
	$M = N - 1$	2	53.066	53.034	53.011	52.994	52.892
		3	53.066	53.034	53.011	52.994	52.982
		4	82.367	82.322	82.290	82.266	82.249
		5	102.410	102.349	102.307	102.276	102.253
	GDQ	1	23.124	23.124	23.124	23.124	23.124
		2	52.917	52.917	52.917	52.917	52.917
		3	52.917	52.917	52.917	52.917	52.917
		4	82.159	82.159	82.159	82.159	82.159
		5	102.135	102.135	102.135	102.135	102.135

differential matrix (after boundary conditions being implemented), $D_q^{R(m)}$, is obtained. Here, $D_q^{R(m)}$ is a $(N-2) \times (N-2)$ differential matrix, q is the direction of differentiation $(q = x, y)$ and m is the order of differentiation. The superscript R is introduced to avoid confusion in notation with $D_q^{(m)}$.

Consider a plate that is discretized into $N \times N$ grid points with M ghost points extended from each edge. The matrix $D_q^{R(m)}$ represents the differential operator for a row or a column in the q direction $(q = x, y)$. For elastic and mixed boundary conditions, different row or column has different a_i and hence requires a different $D_q^{R(m)}$. An array of matrices, $D_q^{VR(m)}$, can be defined to take into account for this complication,

$$D_q^{VR(m)} = [D_{q,0}^{R(m)}, \ldots, D_{q,k}^{R(m)}, \ldots, D_{q,N-1}^{R(m)}]. \tag{44}$$

Table 3
Convergence study: an SESE plate ($K' = 10$, $\lambda = 1$)
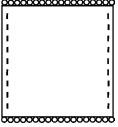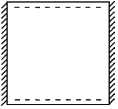
Plate	Method	Ω	$N = 16$	$N = 18$	$N = 20$	$N = 22$	$N = 24$
	DSC-LK with	1	21.520	21.513	21.508	21.504	21.501
	$M = 14$	2	50.006	50.000	49.996	49.993	49.991
		3	52.425	52.398	52.379	52.366	52.355
		4	80.666	80.643	80.627	80.616	80.607
		5	99.021	99.016	99.012	99.009	99.007
	DSC-LK with	1	21.520	21.513	21.508	21.504	21.501
	$M = N - 1$	2	50.006	50.000	49.996	49.993	49.991
		3	52.425	52.398	52.380	52.366	52.355
		4	80.666	80.643	80.627	80.616	80.607
		5	99.021	99.016	99.012	99.009	99.007
	GDQ	1	21.487	21.487	21.487	21.487	21.487
		2	49.980	49.980	49.980	49.980	49.980
		3	52.302	52.302	52.302	52.302	52.302
		4	80.562	80.562	80.562	80.562	80.562
		5	98.996	98.997	98.997	98.997	98.997

Table 4
Convergence study: a CSCS plate ($\lambda = 1$)

Plate	Method	Ω	$N = 16$	$N = 18$	$N = 20$	$N = 22$	$N = 24$
	DSC-LK with	1	28.956	28.955	28.953	28.953	28.952
	$M = 14$	2	54.754	54.751	54.748	54.747	54.746
		3	69.358	69.349	69.342	69.338	69.336
		4	94.636	94.620	94.610	94.604	94.600
		5	102.235	102.229	102.225	102.223	102.221
	DSC-LK with	1	28.956	28.954	28.953	28.953	28.953
	$M = N - 1$	2	54.754	54.749	54.747	54.747	54.747
		3	69.359	69.344	69.344	69.340	69.337
		4	94.638	94.613	94.606	94.606	94.601
		5	102.235	102.226	102.223	102.224	102.222
	GDQ	1	28.951	28.951	28.951	28.951	28.951
		2	54.743	54.743	54.743	54.743	54.743
		3	69.327	69.327	69.327	69.327	69.327
		4	94.585	94.585	94.585	94.585	94.585
		5	102.216	102.216	102.216	102.216	102.216

Denote $[D_q^{VR(m)}]_k = D_{q,k}^{R(m)}$, which is the differential matrix for the kth row (or column), and thus, the matrix element at the ith row and the jth column of $[D_q^{VR(m)}]_k$ is written as $[D_q^{VR(m)}]_{k,(i,j)}$.

With Eq. (44), the governing Eq. (2) for plate vibration can be discretized as

$$\left(D_x^{VR(4)} \dot\otimes I_y + 2\lambda^2 D_x^{VR(2)} \dot\otimes D_y^{VR(2)} + \lambda^4 I_x \dot\otimes D_y^{VR(4)}\right)W = \Omega^2 W, \tag{45}$$

where I_q is a vector of identity matrices (with $q = x, y$), $\dot\otimes$ is defined as contractive tensor product of two vectors of matrices such that $H = A \dot\otimes B$ is

$$H_{(i-1)\times(N-2)+k,(j-1)\times(N-2)+l} = \left(A \dot\otimes B\right)_{i,j,k,l} = A_{k,(i,j)}B_{i,(k,l)} \tag{46}$$

Table 5
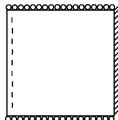Convergence study: a CEES plate ($K' = 10$, $\lambda = 1$)
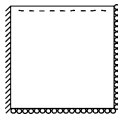
Plate	Method	Ω	$N = 16$	$N = 18$	$N = 20$	$N = 22$	$N = 24$
	DSC-LK with	1	25.480	25.472	25.466	25.462	25.459
	$M = 14$	2	53.578	53.561	53.548	53.539	53.333
		3	60.599	60.577	60.562	60.551	60.543
		4	87.929	87.899	87.879	87.864	87.853
		5	102.349	102.314	102.290	102.262	102.258
	DSC-LK with	1	25.481	25.472	25.466	25.462	25.459
	$M = N - 1$	2	53.579	53.562	53.549	53.540	53.333
		3	60.602	60.579	60.564	60.552	60.544
		4	87.933	87.903	87.881	87.866	87.854
		5	102.351	102.316	102.291	102.273	102.259
	GDQ	1	25.443	25.443	25.443	25.443	25.443
		2	53.499	53.499	53.499	53.499	53.499
		3	60.502	60.502	60.502	60.502	60.502
		4	87.799	87.799	87.799	87.799	87.799
		5	102.191	102.191	102.191	102.191	102.191

Table 6
Convergence study: an SECE plate ($K' = 10$, $\lambda = 1$)

Plate	Method	Ω	$N = 16$	$N = 18$	$N = 20$	$N = 22$	$N = 24$
	DSC-LK with	1	25.172	25.165	25.160	25.156	25.153
	$M = 14$	2	54.662	54.634	54.615	54.601	54.590
		3	59.240	59.231	59.225	59.221	59.218
		4	87.791	87.762	87.743	87.729	87.718
		5	104.016	103.952	103.908	103.876	103.852
	DSC-LK with	1	25.172	25.165	25.160	25.156	25.154
	$M = N - 1$	2	54.662	54.635	54.615	54.601	54.590
		3	59.241	59.232	59.226	59.222	59.218
		4	87.792	87.763	87.744	87.729	87.719
		5	104.016	103.953	103.909	103.876	103.852
	GDQ	1	25.140	25.140	25.140	25.140	25.140
		2	54.536	54.536	54.536	54.536	54.536
		3	59.204	59.204	59.204	59.204	59.204
		4	87.668	87.668	87.668	87.668	87.668
		5	103.730	103.731	103.731	103.731	103.731

and W is a column vector such that

$$[W] = [W_{1,1}, \ldots, W_{1,N-2}, W_{2,1}, \ldots, W_{N-2,N-2}]^{\mathrm{T}}. \tag{47}$$

Table 7
Solutions and percent errors of an SSSS plate ($N = 32$, $M = 31$, $\lambda = 1$)

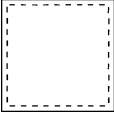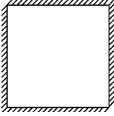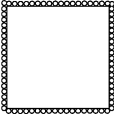| Ω	Exact [1]	DSC-LK	GDQ	% Error (DSC)	% Error (GDQ)
1	19.7392088022	19.7392088078	19.7392088001	$+2.87 \times 10^{-8}$	-1.08×10^{-8}
2	49.3480220054	49.3480220055	49.3480220048	$+1.30 \times 10^{-10}$	-1.29×10^{-9}
3	49.3480220054	49.3480220055	49.3480220084	$+1.30 \times 10^{-10}$	$+5.98 \times 10^{-9}$
4	78.9568352087	78.9568352082	78.9568352139	-6.16×10^{-10}	$+6.55 \times 10^{-9}$
5	98.6960440109	98.6960440042	98.6960440102	-6.76×10^{-9}	-6.81×10^{-10}
6	98.6960440109	98.6960440111	98.6960440127	$+2.51 \times 10^{-10}$	$+1.80 \times 10^{-9}$
7	128.304857214	128.304857215	128.304857214	$+2.93 \times 10^{-10}$	-4.54×10^{-10}
8	128.304857214	128.304857219	128.304857215	$+3.59 \times 10^{-9}$	$+7.42 \times 10^{-10}$
9	167.783274819	167.783274818	167.783274817	-2.86×10^{-10}	-1.16×10^{-9}
10	167.783274819	167.783274819	167.783274819	$+5.45 \times 10^{-10}$	$+3.17 \times 10^{-10}$
20	315.827340835	315.827340833	315.827340836	-4.78×10^{-10}	$+5.10 \times 10^{-10}$
30	444.132198049	444.132198050	444.132198049	$+2.08 \times 10^{-10}$	$+6.06 \times 10^{-11}$
40	602.045868466	602.045868465	602.045868467	-1.68×10^{-10}	$+1.07 \times 10^{-11}$
50	720.481121280	720.481121280	720.481120058	$+4.15 \times 10^{-11}$	-1.69×10^{-7}
60	838.916374093	838.916374093	838.916448905	$+9.76 \times 10^{-12}$	$+8.92 \times 10^{-6}$
70	996.830044510	996.830044510	996.830888933	-6.28×10^{-12}	$+8.47 \times 10^{-5}$
80	1144.87411053	1144.87411053	1144.87484158	$+6.93 \times 10^{-13}$	$+6.39 \times 10^{-5}$
90	1263.30936334	1263.30936334	1263.30936197	$+2.05 \times 10^{-11}$	-1.08×10^{-7}
100	1431.09263816	1431.09263816	1430.97631413	$+5.66 \times 10^{-13}$	-8.13×10^{-3}
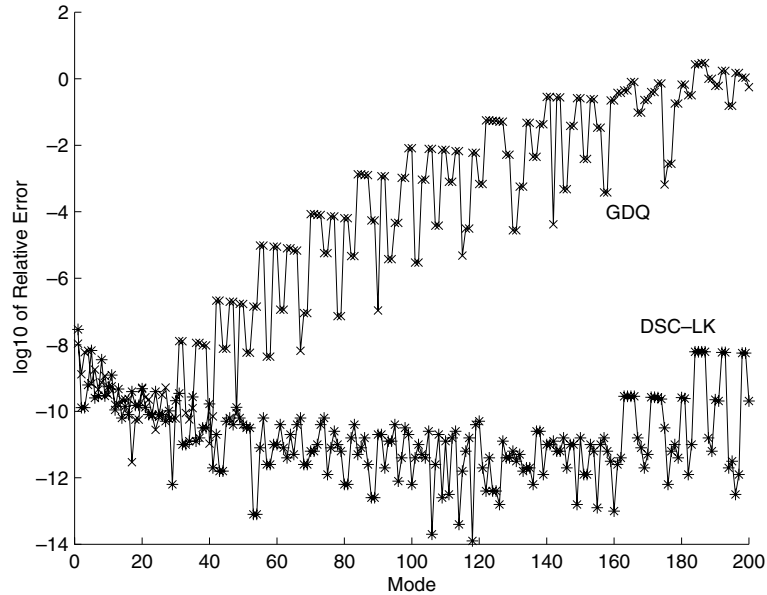
Fig. 2. Comparison of errors by the DSC-LK and GDQ methods for an SSSS plate ($N = 32$).

Table 8
Comparison study on homogeneous plates ($N = 24$, $M = 23$, $\lambda = 1$, $K' = 10$)

| Plate	Ω	Leissa [1,2]	DSC-LK	GDQ	% Diff(L)	% Diff(GDQ)
	1	*19.739*	19.739	19.739	0.000	0.000
	2	*49.348*	49.348	49.348	0.000	0.000
	3	*49.348*	49.348	49.348	0.000	0.000
	4	*78.957*	78.957	78.957	0.000	0.000
	5	*98.696*	98.696	98.696	0.000	0.000
	6	*98.696*	98.696	98.696	0.000	0.000
	7	*128.305*	128.305	128.305	0.000	0.000
	8	*128.305*	128.305	128.305	0.000	0.000
	1	35.992	35.989	35.985	−0.008	0.009
	2	73.413	73.407	73.394	−0.008	0.018
	3	73.413	73.407	73.394	−0.008	0.018
	4	108.27	108.249	108.210	−0.019	0.030
	5	131.64	131.622	131.580	−0.014	0.031
	6	132.24	132.244	132.200	0.003	0.029
	7	–	165.074	165.000	–	0.045
	8	–	165.074	165.000	–	0.045
	1	–	23.152	23.124	–	0.121
	2	–	52.892	52.917	–	0.123
	3	–	52.892	52.917	–	0.123
	4	–	82.249	82.159	–	0.109
	5	–	102.253	102.136	–	0.115
	6	–	102.971	102.828	–	0.138
	7	–	131.677	131.535	–	0.108
	8	–	131.677	131.535	–	0.108
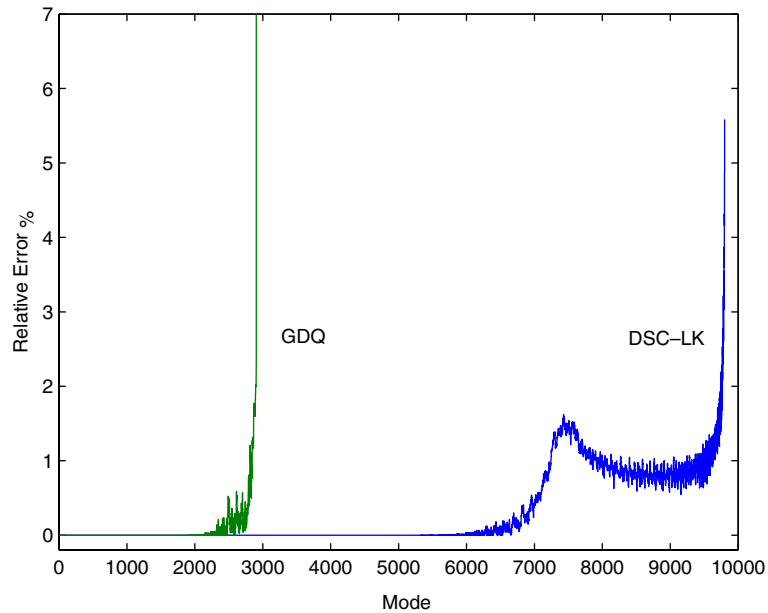
Fig. 3. Comparison of errors by the DSC-LK and GDQ methods for an SSSS plate ($N = 101$).

Eq. (45) can be expressed as a problem of eigenvalue and eigenvector

$$[A][W] = \Omega^2[W]. \tag{48}$$

The eigenvalue Ω^2 can be obtained by solving Eq. (48) with a standard eigenvalue solver.

3. Results and discussions

The numerical results of the GDQ and DSC-LK are presented and discussed in this section. The DSC-LK is implemented on uniform grids. However, to maintain the numerical stability, the GDQ has to be implemented on shifted Chebyshev–Gauss–Lobatto grids [37–40]

$$x_i = \frac{1}{2}\left[1 - \cos\left(\frac{i-1}{N-1}\pi\right)\right] \quad \text{for } i = 1, 2, \ldots, N, \tag{49}$$

$$y_j = \frac{1}{2}\left[1 - \cos\left(\frac{j-1}{N-1}\pi\right)\right] \quad \text{for } j = 1, 2, \ldots, N. \tag{50}$$

For the convenience of discussion and comparison, the following terminology is defined for the frequency parameter $\Omega = \omega a^2(\rho h/D)^{1/2}$

$$\text{Error(DSC)} = \frac{\text{DSC-LK's result} - \text{Exact result}}{\text{Exact result}} \times 100\%, \tag{51}$$

Table 9
Comparison study on homogeneous plates ($N = 24$, $M = 23$, $\lambda = 1$, $K' = 10$)

Plate	Ω	Leissa [1,2]	DSC-LK	GDQ	% Diff(L)	% Diff(GDQ)
	1	*23.646*	23.647	23.646	0.003	0.002
	2	*51.674*	51.675	51.674	0.001	0.002
	3	*58.646*	58.650	58.646	0.006	0.006
	4	*86.135*	86.141	86.134	0.008	0.007
	5	*100.270*	100.272	100.270	0.002	0.002
	6	*113.228*	113.241	113.228	0.011	0.011
	7	*133.791*	133.801	133.791	0.007	0.008
	8	*140.846*	140.864	140.846	0.013	0.013
	1	–	20.597	20.591	–	0.032
	2	–	49.664	49.658	–	0.011
	3	–	50.850	50.824	–	0.051
	4	–	79.777	79.755	–	0.027
	5	–	98.850	98.845	–	0.005
	6	–	100.500	100.842	–	0.058
	7	–	128.807	128.786	–	0.016
	8	–	129.487	129.438	–	0.038
	1	31.829	31.828	31.826	−0.003	0.007
	2	63.347	63.338	63.331	−0.014	0.011
	3	71.084	71.087	71.076	0.004	0.006
	4	100.83	100.815	100.792	−0.015	0.022
	5	116.40	116.376	116.357	−0.021	0.016
	6	130.37	130.388	130.351	0.014	0.028
	7	–	151.938	151.893	–	0.030
	8	–	159.534	159.476	–	0.036

$$\text{Error(GDQ)} = \frac{\text{GDQ's result} - \text{Exact result}}{\text{Exact result}} \times 100\%, \tag{52}$$

$$\text{Diff(L)} = \frac{\text{DSC-LK's result} - \text{Leissa's result}}{\text{Leissa's result}} \times 100\%, \tag{53}$$
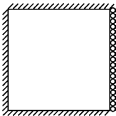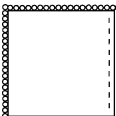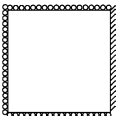
$$\text{Diff(GDQ)} = \frac{\text{DSC-LK's result} - \text{GDQ's result}}{\text{GDQ's result}} \times 100\%. \tag{54}$$

3.1. Convergence study

This section presents the convergence study (see Tables 1–6) of six different plates. These six plates are selected to cover the following six cases:

- Single uniform boundary condition (SSSS plate);
- Single non-uniform boundary condition (EEEE plate);
- Combination of two different boundary conditions (one of them is non-uniform) (SESE plate);
- Combination of two different boundary conditions (both are uniform) (SCSC plate);
- Combination of three different boundary conditions (SEEC plate);
- Combination of three different boundary conditions (with one pair of elastic support on opposing edges) (SECE plate).

Table 10
Comparison study on homogeneous plates ($N = 24$, $M = 23$, $\lambda = 1$, $K' = 10$)

Plate	Ω	Leissa [1,2]	DSC-LK	GDQ	% Diff(L)	% Diff(GDQ)
	1	–	32.684	32.676	–	0.033
	2	–	64.894	64.854	–	0.061
	3	–	71.407	71.389	–	0.025
	4	–	101.676	101.626	–	0.049
	5	–	118.245	118.156	–	0.076
	6	–	130.546	130.504	–	0.033
	7	–	153.197	153.092	–	0.069
	8	–	160.053	159.970	–	0.052
	1	–	22.302	22.282	–	0.092
	2	–	51.485	51.447	–	0.073
	3	–	52.663	52.604	–	0.112
	4	–	81.423	81.356	–	0.082
	5	–	100.423	100.704	–	0.067
	6	–	102.494	102.368	–	0.123
	7	–	130.493	130.402	–	0.070
	8	–	131.173	131.053	–	0.092
	1	–	26.213	26.189	–	0.089
	2	–	54.990	54.929	–	0.112
	3	–	60.830	60.782	–	0.078
	4	–	88.647	88.569	–	0.088
	5	–	104.046	103.918	–	0.123
	6	–	115.398	115.305	–	0.081
	7	–	136.732	136.595	–	0.101
	8	–	143.081	142.962	–	0.083

For each of the above cases, the DSC-LK (for $M = 14$ and $M = N - 1$) and GDQ are implemented on a grid size varying from $N = 16$ to $N = 24$. The DSC-LK exhibits excellent convergence for the SSSS plate. The results of the DSC-LK converge to five significant figures for a small grid size of $N = 16$. For the remaining five plates, the DSC-LK demonstrates good convergence for the first five eigenfrequencies. On the other hand, the GDQ shows excellent convergence for all the six plates. In all the six plates, the results of the GDQ converge to five significant figures for a small grid size of $N = 18$.
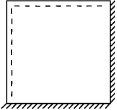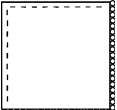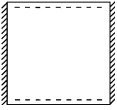
From the convergence study of the six plates, we can conclude that the DSC-LK shows very good convergence for the first five eigenfrequencies, whereas the GDQ shows even better convergence than the DSC-LK. This difference in speed of convergence is due to the fact that the GDQ utilizes a non-uniform grid. It is found that the results of the GDQ obtained on a uniform grid are not as good as those of the DSC-LK (results are not shown).

It is worth mentioning that for grid size $N = n$, the DSC and GDQ will produce $(n - 2)^2$ by $(n - 2)^2$ matrix and $(n - 4)^2$ by $(n - 4)^2$ matrix respectively. Hence the GDQ produces slightly smaller matrix as compared to the DSC. Furthermore, it is observed that the DSC generally produces upper bound, monotonic convergence.

3.2. Comparison study on higher-order eigenfrequencies

High frequency vibration prediction is a challenging task in structural analysis and optimization. The prediction is of particular importance for aerospace structures, such as aircrafts, jets, satellites and space shuttles, which are subject to various high frequency excitations. This subsection studies the accuracy of the DSC-LK and GDQ for higher-order eigenfrequencies of an SSSS plate. The numerical results for the first

Table 11
Comparison study on homogeneous plates ($N = 24$, $M = 23$, $\lambda = 1$, $K' = 10$)

Plate	Ω	Leissa [1,2]	DSC-LK	GDQ	% Diff(L)	% Diff(GDQ)
	1	27.056	27.055	27.054	−0.004	0.004
	2	60.544	60.543	60.538	−0.002	0.008
	3	60.791	60.791	60.786	0.000	0.008
	4	92.865	92.849	92.836	−0.017	0.014
	5	114.57	114.572	114.550	0.002	0.014
	6	114.72	114.719	114.704	−0.001	0.013
	7	–	145.811	145.781	–	0.021
	8	–	146.109	146.080	–	0.020
	1	–	21.426	21.413	–	0.061
	2	–	51.139	51.108	–	0.060
	3	–	51.184	51.152	–	0.063
	4	–	80.595	80.551	–	0.054
	5	–	100.47	100.413	–	0.057
	6	–	100.838	100.768	–	0.070
	7	–	129.978	129.909	–	0.053
	8	–	129.999	129.928	–	0.055
	1	*28.951*	28.953	28.951	0.007	0.006
	2	*54.743*	54.747	54.743	0.007	0.006
	3	*69.327*	69.337	69.327	0.014	0.014
	4	*94.585*	94.601	94.585	0.017	0.017
	5	*102.21*	102.222	102.216	0.012	0.006
	6	*129.09*	129.130	129.096	0.031	0.026
	7	*140.20*	140.230	140.205	0.021	0.018
	8	*154.77*	154.823	154.776	0.034	0.030

10 eigenfrequencies as well as the 20th, 30th, 40th, 50th, 60th, 70th, 80th, 90th, 100th eigenfrequencies are tabulated in Table 7.
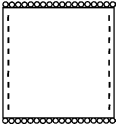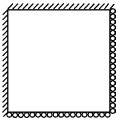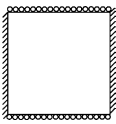
For the first 10 eigenfrequencies, the GDQ is more accurate than the DSC-LK for the 1st, 5th, 8th and 10th eigenfrequencies while the DSC-LK is more accurate for the 2nd, 3rd, 4th, 6th, 7th and 9th eigenfrequencies. Generally, for the first 49 eigenfrequencies, both the GDQ and DSC-LK have similar level of accuracy as one is more accurate for certain eigenfrequencies while the other is more accurate for the rest. The results of the DSC-LK have $6.2 \times 10^{-13}\%$ to $2.9 \times 10^{-8}\%$ absolute relative error while the results of the GDQ have $3.0 \times 10^{-12}\%$ to $2.14 \times 10^{-7}\%$ absolute relative error. The small absolute relative errors of the DSC-LK for the first 49 eigenfrequencies correspond to at least 10 significant figure accuracy.

For the 50th to 150th eigenfrequencies, the results of the DSC-LK are significantly more accurate than those of the GDQ (see Fig. 2). The results of the DSC-LK have $1.4 \times 10^{-14}\%$ to $6.6 \times 10^{-11}\%$ absolute relative error while the results of the GDQ have $4.4 \times 10^{-9}\%$ to $2.8 \times 10^{-1}\%$ absolute relative error. The small absolute relative errors of the DSC-LK for the 50th to the 150th eigenfrequencies correspond to at least 12 significant figure accuracy.

It is observed (see Fig. 2) that the error of the GDQ increases rapidly from the 50th eigenfrequency onward. The use of non-uniform grid may be the cause for such an increase. Non-uniform grid helps to enhance the stability and accuracy [40] of the GDQ method but it has relatively fewer grid points at the center of the computational domain. At higher eigenfrequencies, the high frequency component at the center of the plate may not be accurately approximated by the relatively smaller number of grid points at the center of the plate. This inaccuracy in approximation may in turn increases the error of the GDQ.

All the values in Table 8 and Fig. 2 are computed by using $N = 32$ grid points. Therefore the *Nyquist frequency* is 16 wavelengths. In Fig. 2, the $(15, 1)$ mode corresponds to 163th eigenfrequency while the

Table 12
Comparison study on homogeneous plates ($N = 24$, $M = 23$, $\lambda = 1$, $K' = 10$)

Plate	Ω	Leissa [1,2]	DSC-LK	GDQ	% Diff(L)	% Diff(GDQ)
	1	*21.235*	21.501	21.487	1.254	0.067
	2	–	49.991	49.980	–	0.023
	3	–	52.355	52.302	–	0.102
	4	–	80.607	80.562	–	0.055
	5	–	99.007	98.997	–	0.010
	6	–	102.301	102.182	–	0.116
	7	–	129.313	129.271	–	0.033
	8	–	130.673	130.574	–	0.076
	1	–	28.987	28.968	–	0.067
	2	–	62.598	62.555	–	0.069
	3	–	62.623	62.576	–	0.074
	4	–	94.646	94.580	–	0.071
	5	–	116.617	116.532	–	0.073
	6	–	116.748	116.650	–	0.084
	7	–	147.747	147.629	–	0.080
	8	–	147.797	147.688	–	0.074
	1	32.179	30.236	30.222	−6.038	0.046
	2	–	57.575	57.519	–	0.098
	3	–	69.839	69.819	–	0.029
	4	–	96.099	96.039	–	0.063
	5	–	105.807	105.680	–	0.120
	6	–	129.395	129.351	–	0.034
	7	–	142.562	142.433	–	0.090
	8	–	155.720	155.632	–	0.057

(16, 1) mode corresponds to 184th eigenfrequency. Fig. 2 shows that the results of the DSC-LK have at least 10 significant figures accuracy up to the 184th eigenfrequency. Here (m, n) represents the mode having m and n half waves in the x and y directions, respectively.

From the comparison study of the SSSS plate, we can conclude that the DSC-LK is significantly more accurate than the GDQ for the analysis of higher-order eigenfrequencies. More comparison is available in Fig. 3.

3.3. Comparison study on numerical stability

Numerical stability is a crucial issue for a computational method. Many p-version finite element methods used for structural analyses are numerically unstable as the degree of polynomial increases. Numerical instability is due to computer's round-off errors in computing high order polynomial coefficients and matrix elements. Such round-off errors lead to ill-conditioned mass and stiffness matrices. The GDQ method has a similar problem in handling large scale computations as its degree of polynomial is tied up with its number of grid points. The use of uniform grids adds to the instability. Numerical instability leads to complex eigenvalues for the higher-order eigenfrequencies of the GDQ results. In this subsection, we investigate the numerical stability of the GDQ and DSC-LK methods. All results are calculated in double precision.

Fig. 3 depicts the relative errors of both the GDQ and DSC-LK for the SSSS plate. The GDQ method ($N = 101$) gives a correct prediction for the first 2700 eigenfrequencies and diverges beyond such a point. In contrast, on the same grid with $M = 100$, the DSC-LK gives a correct prediction with errors less than 5% for modal number up to 9800. Because of the use of a large M these results are significantly better than

Table 13
Comparison study on homogeneous plates ($N = 24$, $M = 23$, $\lambda = 1$, $K' = 10$)

Plate	Ω	Leissa [1,2]	DSC-LK	GDQ	% Diff(L)	% Diff(GDQ)
	1	–	24.377	24.370	–	0.027
	2	–	53.129	53.102	–	0.051
	3	–	58.930	58.921	–	0.015
	4	–	86.924	86.896	–	0.032
	5	–	102.065	102.004	–	0.060
	6	–	113.386	113.368	–	0.016
	7	–	134.976	134.915	–	0.045
	8	–	141.340	141.300	–	0.028
	1	–	24.753	24.742	–	0.042
	2	–	52.083	52.074	–	0.017
	3	–	60.268	60.232	–	0.060
	4	–	87.074	87.040	–	0.038
	5	–	100.467	100.458	–	0.009
	6	–	115.103	115.021	–	0.071
	7	–	134.379	134.344	–	0.027
	8	–	142.130	142.054	–	0.054
	1	–	28.031	28.021	–	0.037
	2	–	61.027	61.015	–	0.020
	3	–	62.253	62.216	–	0.060
	4	–	93.750	93.710	–	0.042
	5	–	114.821	114.800	–	0.019
	6	–	116.505	116.421	–	0.073
	7	–	146.500	146.444	–	0.038
	8	–	147.234	147.147	–	0.059

those of a previous work [56] obtained by using the DSC-regularized Shannon kernel ($M = 32$). The DSC-LK results are some of the best results even available for this problem.
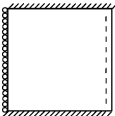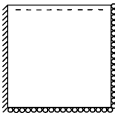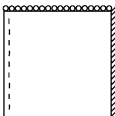
It is noted that in the DSC-LK algorithm, the total number of grid points used in each dimension (N) is disconnected from the number of weight coefficients ($2M + 1$), or computational bandwidth. Therefore, one can use arbitrary number of grid points (N) with a relatively small M value in the numerical computation. As such, one can further gain the access to large scale computations with the numerical stability by using the DSC algorithm.

3.4. Comparison study on all combinations of 21 homogeneous plates

Both the DSC-LK and GDQ are implemented on transversely vibrating plates with simply supported (S), clamped (C), and transversely supported with non-uniform elastic rotational restraint (E) edges. A total of 21 cases (see Tables 8–14) with different boundary conditions are studied. For each case, the first 8 eigenfrequencies are calculated with $N = 24$, $M = 23$, $\lambda = 1$ and $K' = 10$. These 21 cases represent all the possible combinations for the above three types of support edges, including four plates that have exact solutions, i.e. the SSSS, SSSC, SCSC and SESE plates (in Tables 8, 9, 11 and 12 respectively). These exact results given by Leissa [1,2] are listed in italic in the tables.

For the SSSS, SSSC and SCSC plates, the results of the DSC-LK agree very well with the exact solutions with less than 0.04% absolute relative error. On the other hand, the results of the GDQ agree extremely well with the exact solutions [1]. The maximum relative difference between the DSC-LK and GDQ methods is just 0.03%. For the SESE plate, both the results of the DSC-LK and GDQ agree with the exact solution [2]

Table 14
Comparison study on homogeneous plates ($N = 24$, $M = 23$, $\lambda = 1$, $K' = 10$)

Plate	Ω	Leissa [1,2]	DSC-LK	GDQ	% Diff(L)	% Diff(GDQ)
	1	–	29.571	29.564	–	0.024
	2	–	56.156	56.127	–	0.052
	3	–	69.583	69.568	–	0.021
	4	–	95.345	95.307	–	0.040
	5	–	104.016	103.951	–	0.063
	6	–	129.261	129.222	–	0.030
	7	–	141.393	141.317	–	0.054
	8	–	155.269	155.201	–	0.043
	1	–	25.459	25.443	–	0.064
	2	–	53.533	53.499	–	0.064
	3	–	60.544	60.502	–	0.069
	4	–	87.854	87.799	–	0.063
	5	–	102.259	102.191	–	0.066
	6	–	115.248	115.161	–	0.076
	7	–	135.553	135.467	–	0.063
	8	–	142.603	142.506	–	0.068
	1	–	25.154	25.140	–	0.055
	2	–	54.590	54.536	–	0.099
	3	–	59.218	59.204	–	0.024
	4	–	87.719	87.668	–	0.058
	5	–	103.852	103.731	–	0.117
	6	–	113.535	113.511	–	0.021
	7	–	136.156	136.045	–	0.082
	8	–	141.818	141.757	–	0.043

within less than 1.3% absolute relative error. The relative difference between the DSC-LK and GDQ methods is 0.12%.

From the comparison study of the four plates, we see that the results of the DSC-LK agree well with the exact solutions, whereas the GDQ is more accurate. The results of the GDQ are significantly more accurate than those of the DSC-LK for the SSSS, SSSC and SCSC plates due to the use of non-uniform grids. However, the GDQ is only slightly more accurate than the DSC-LK for the SESE plate. This might be due to the fact that the non-uniform rotational spring coefficient $K(s)$ attains its maximum at the middle of the plate edge where the grid points are very sparse in the GDQ approach.

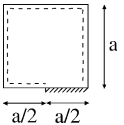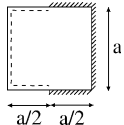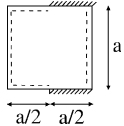Table 15
Comparison study on mixed plates ($N = 24$, $M = 23$)

Plate	Method	Ω_1	Ω_2	Ω_3	Ω_4	Ω_5
	Nowacki [10]	22.4	–	–	–	–
	Cheung [11]	22.5	–	–	–	–
	Keer and Stahl [12]	22.49	–	–	–	–
	Rao et al. [13]	22.96	–	–	–	–
	Narita [14]	22.63	50.04	55.95	82.34	99.71
	Gorman [15]	22.48	–	–	–	–
	Fan and Cheung [4]	22.73	50.15	56.23	–	–
	Mizusawa and Leonard [16]	22.71	50.10	56.13	82.37	99.73
	Liew et al. [17]	22.40	–	–	–	–
	DSC-LK	22.39	49.86	55.47	82.26	99.66
	GDQ	22.43	49.93	55.53	82.30	99.65
	Piskunov [18]	26.3	–	–	–	–
	Cheung [11]	28.1	–	–	–	–
	Fan and Cheung [4]	28.65	61.06	62.48	–	–
	Mizusawa and Leonard [16]	28.56	61.01	62.23	94.53	113.40
	DSC-LK	27.73	60.27	61.00	94.55	111.72
	GDQ	27.86	60.57	61.00	94.49	112.13
	Ota and Hamada [19]	25.5	–	–	–	–
	Cheung [11]	25.9	–	–	–	–
	Fan and Cheung [4]	26.37	52.23	61.8	–	–
	DSC-LK	25.51	52.09	59.63	88.15	100.53
	GDQ	25.62	52.13	59.89	88.13	100.50

Table 16
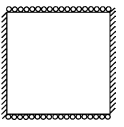Comparison study on CECE plate ($N = 24$, $M = 23$)

Plate	λ	K'	Leissa [2]	DSC-LK	GDQ	% Diff(L)	% Diff(GDQ)
	0.5	0.1	23.844	23.819	23.818	−0.105	0.004
		1	23.876	23.84	23.839	−0.151	0.004
		10	24.136	24.002	23.996	−0.555	0.025
		100	24.561	24.405	24.393	−0.635	0.049
	1	0.1	28.969	28.968	28.966	−0.003	0.007
		1	29.219	29.105	29.103	−0.390	0.007
		10	32.179	30.236	30.222	−6.038	0.046
		100	35.379	33.849	33.796	−4.325	0.157

Table 17
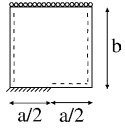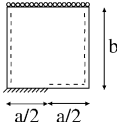Comparison study on mixed and non-uniform plates ($N = 24$, $M = 23$)

Plate	λ	K'	Ω	DSC-LK	GDQ	% Diff(GDQ)
	0.5	0.1	1	14.964	14.989	−0.167
			2	22.045	22.043	0.009
			3	33.763	33.722	0.122
			4	45.543	45.550	−0.015
			5	50.503	50.475	0.055
		1	1	15.116	15.140	−0.159
			2	22.146	22.143	0.014
			3	33.820	33.778	0.124
			4	45.704	45.708	−0.009
			5	50.546	50.519	0.053
		10	1	16.257	16.278	−0.129
			2	22.972	22.959	0.057
			3	34.301	34.25	0.149
			4	47.061	47.035	0.055
			5	50.916	50.896	0.039
		100	1	18.994	19.009	−0.079
			2	25.562	25.516	0.180
			3	36.032	35.950	0.228
			4	51.293	51.130	0.319
			5	52.962	52.995	−0.062

Table 18
Comparison study on mixed and non-uniform plates ($N = 24$, $M = 23$)

Plate	λ	K'	Ω	DSC-LK	GDQ	% Diff(GDQ)
	1	0.1	1	22.406	22.444	−0.169
			2	49.864	49.931	−0.134
			3	55.490	55.544	−0.097
			4	82.265	82.311	−0.056
			5	99.660	99.649	0.011
		1	1	22.517	22.556	−0.173
			2	49.914	49.979	−0.130
			3	55.636	55.688	−0.093
			4	82.356	82.400	−0.053
			5	99.678	99.666	0.012
		10	1	23.406	23.439	−0.141
			2	50.328	50.381	−0.105
			3	56.901	56.937	−0.063
			4	83.169	83.187	−0.022
			5	99.839	99.822	0.017
		100	1	25.885	25.906	−0.081
			2	51.794	51.811	−0.033
			3	61.697	61.673	0.039
			4	86.825	86.737	0.101
			5	100.629	100.585	0.044

It is observed that the results from Leissa, DSC-LK and GDQ have very good agreement for fully simply supported plate. Difference in the results of the DSC-LK with those of Leissa and GDQ becomes larger for elastic edges and clamped edges. The largest difference in Diff(L) occurs in the CECE plate with Diff(L) = −6.1% and Diff(GDQ) = 0.046%. The largest difference in Diff(GDQ) occurs in the fully elastic plate with Diff(GDQ) = 0.14%. After all, these differences are still acceptable for structural analysis.

From the comparison study of the 21 homogeneous plates, we can conclude that the results of the DSC-LK agree well with those of Leissa and GDQ. The performance of two methods on plates with mixed edge supports is examined in Section 3.5.

3.5. Comparison study on three plates with mixed boundary condition

In this subsection, the DSC-LK and GDQ are implemented on three plates with mixed boundary conditions (see Table 15). Both methods are compared with some previous approaches. The numerical results for the DSC-LK and GDQ agree satisfactorily with the existing literature as shown in Table 15.

3.6. Comparison study on three plates with elastic supports

For a better understanding of the DSC-LK and GDQ with application to non-uniform elastic rotational restraint (E) edges, another three plates (see Table 16–20) with elastic edges are considered. A range of aspect ratios ($\lambda = 0.5$ and 1) and non-dimensional spring coefficients ($K' = 0.1$, 1, 10 and 100) are tested. The first plate is a CECE plate. The results of the DSC-LK agree satisfactorily with those of Leissa et al. [2] and the results of the GDQ with less than 6.1% and 0.16% absolute relative difference respectively. For CECE plates, it is observed that the absolute relative difference between the results of the DSC-LK and those of the GDQ generally increases with λ and K'. The second and third plates have mixed non-uniform

Table 19
Comparison study on mixed and non-uniform plates ($N = 24$, $M = 23$)

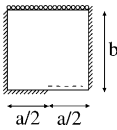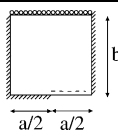| Plate	λ	K'	Ω	DSC-LK	GDQ	% Diff(GDQ)
	0.5	0.1	1	16.391	16.366	0.153
			2	25.500	25.493	0.027
			3	40.115	40.095	0.050
			4	46.687	46.63	0.122
			5	57.449	57.438	0.019
		1	1	16.543	16.516	0.163
			2	25.589	25.582	0.027
			3	40.166	40.146	0.05
			4	46.856	46.797	0.126
			5	57.597	57.583	0.024
		10	1	17.683	17.648	0.198
			2	26.323	26.31	0.049
			3	40.601	40.573	0.069
			4	48.296	48.215	0.168
			5	58.867	58.825	0.071
		100	1	20.400	20.345	0.270
			2	28.600	28.568	0.112
			3	42.146	42.094	0.124
			4	53.346	53.193	0.288
			5	61.026	60.958	0.112

Table 20
Comparison study on mixed and non-uniform plates ($N = 24$, $M = 23$)

Plate	λ	K'	Ω	DSC-LK	GDQ	% Diff(GDQ)
	1	0.1	1	30.986	30.997	−0.035
			2	59.840	59.873	−0.055
			3	70.462	70.449	0.018
			4	96.813	96.791	0.023
			5	110.975	111.019	−0.04
		1	1	31.072	31.082	−0.032
			2	59.987	60.018	−0.052
			3	70.495	70.482	0.018
			4	96.900	96.875	0.026
			5	111.147	111.185	−0.034
		10	1	31.754	31.759	−0.016
			2	61.245	61.25	−0.008
			3	70.792	70.773	0.027
			4	97.673	97.624	0.05
			5	112.689	112.671	0.016
		100	1	33.703	33.693	0.03
			2	65.687	65.622	0.099
			3	72.082	72.035	0.065
			4	101.04	100.896	0.143
			5	119.537	119.318	0.184

boundary conditions. The results of the DSC-LK agree satisfactorily with those of the GDQ with less than 0.32% absolute relative difference.

4. Conclusion

This paper uses Lagrange's delta sequence kernel (LK) for the vibration analysis of plates in the framework of the discrete singular convolution (DSC). A comprehensive comparison between the DSC-LK and the (global) generalized differential quadrature (GDQ) is carried out to study the philosophy of both approaches. The starting point of the DSC algorithm is to construct a sequence of approximations to the delta distribution while the GDQ seeks a differential quadrature by using the global Lagrange interpolation formula. Although both the DSC-LK and GDQ employ the Lagrange kernels, DSC-LK is a local method with a variable computational bandwidth and the GDQ is a global one. The GDQ yields a full matrix for an eigenvalue problem, whereas DSC-LK derives a relatively sparse matrix. Since the total number of grid points does not need to be associated with the matrix band in the DSC-LK, the latter can be easily implemented to a problem which requires a large grid (say hundreds or thousands of grid points in each dimension), whereas the GDQ matrix becomes numerically unstable for such a problem. Unlike the GDQ, which handles boundary conditions by a number of equations, the DSC algorithm employs a set of ficti-tious points to satisfy various boundary conditions. In its evolution, the GDQ has adapted a non-uniform grid to increase its stability and accuracy. A uniform grid DSC-LK is found to be good enough for all problems presented in this work.

To qualitatively compare the performance of the DSC-LK and GDQ, both approaches are implemented on a total of 21 homogeneous plates and 5 plates with mixed boundary condition over a range of aspect ratios and non-dimensional spring coefficients. Numerical experiments show that for the first 8 eigen-

frequencies, the results of the DSC-LK agree well with the existing literature, whereas the GDQ is generally more accurate. For higher order eigenfrequencies, the DSC-LK produces significantly more accurate results than GDQ. The results of the DSC-LK for an SSSS plate have at least 10 significant figure accuracy for the first 49 eigenfrequencies and at least 12 significant figure accuracy for the 50th to 150th eigenfrequencies. Furthermore, the DSC-LK provides correct predictions for the first 9800 eigenfrequencies with 101 grid points in each dimension, whereas the GDQ method encounters numerical instability at mode 2900. Thus, the DSC-LK has a great potential for use in large scale computations. All numerical results indicate that both the GDQ and DSC-LK are very promising approaches for the vibration analysis of plates.

References

[1] A.W. Leissa, The free vibration of rectangular plates, J. Sound Vib. 31 (1973) 257–293.
[2] A.W. Leissa, P.A.A. Laura, R.H. Gutierrez, Vibrations of rectangular plates with non–uniform elastic edge supports, J. Appl. Mech. 47 (1980) 891–895.
[3] A.W. Leissa, Vibration of Plates (NASA SP–160), US Government Printing Office, Washington, DC, 1969.
[4] S.C. Fan, Y.K. Cheung, Flexural free vibrations of rectangular plates with complex support conditions, J. Sound Vib. 93 (1984) 81–94.
[5] C.Y. Chia, Non-linear vibration of anisotropic rectangular plates with non-uniform edge constraints, J. Sound Vib. 101 (1985) 539–550.
[6] H.H.E. Leipholz, On some developments in direct methods of the calculus of variations, Appl. Mech. Rev. 40 (10) (1987) 1379–1392.
[7] P. Zitnan, Vibration analysis of membranes and plates by a discrete least squares technique, J. Sound Vib. 195 (4) (1996) 595–605.
[8] B.M. Donning, W.K. Liu, Meshless methods for shear-deformable beams and plates, Comput. Methods Appl. Mech. Engrg. 152 (1998) 47–71.
[9] T. Belytschko, Y.Y. Lu, L. Gu, Element-free Galerkin methods, Int. J. Numer. Methods Engrg. 37 (1994) 229–256.
[10] W. Nowacki, Free vibrations and buckling of a rectangular plate with discontinuous boundary conditions, Bull. Acad. Pol. Sci. Biol. 3 (1955) 159–167.
[11] M.S. Cheung, Ph.D. thesis, University of Calgary, Finite strip analysis of structures, 1971.
[12] L.M. Keer, B. Stahl, Eigenvalue problems of rectangular plates with mixed edge conditions, J. Appl. Mech. 39 (1972) 513–520.
[13] G.V. Rao, I.S. Raju, T.V.G.K. Murthy, Vibration of rectangular plates with mixed boundary conditions, J. Sound Vib. 30 (1973) 257–260.
[14] Y. Narita, Application of a series-type method to vibration of orthotropic rectangular plates with mixed boundary conditions, J. Sound Vib. 77 (3) (1981) 345–355.
[15] D.J. Gorman, An exact analytical approach to the free vibration analysis of rectangular plates with mixed boundary conditions, J. Sound Vib. 93 (1984) 235–247.
[16] T. Mizusawa, J.W. Leonard, Vibration and buckling of plates with mixed boundary conditions, Engrg. Struct. 12 (1990) 285–290.
[17] K.M. Liew, K.C. Hung, K.Y. Lam, On the use of the substructure method for vibration analysis of rectangular plates with discontinuous boundary conditions, J. Sound Vib. 163 (1993) 451–462.
[18] V.H. Piskunov, Determination of the frequencies of the natural oscillations of rectangular plates with mixed boundary conditions, Prikl. Mekh. 10 (1964) 72–76 (in Ukrainian).
[19] T. Ota, M. Hamada, Fundamental frequencies of simply supported but partially clamped square plates, Bull. Jpn. Soc. Mech. Engrg. 6 (1963) 397–403.
[20] D. Young, Vibration of rectangular plates by the Ritz method, Trans. Amer. Soc. Mech. Engrs.: J. Appl. Mech. 17 (1950) 448–453.
[21] S.P. Timoshenko, S. Woinowsky-Krieger, Theory of Plates and Shells, McGraw-Hill, Singapore, 1970.
[22] S.F. Bassily, S.M. Dickinson, On the use of beam functions for problems of plates involving free edges, Trans. Amer. Soc. Mech. Engrs.: J. Appl. Mech. 42 (1975) 858–864.
[23] T. Mizusawa, T. Kajita, M. Naruoka, Vibration of skew plates by using B-spline functions, J. Sound Vib. 62 (1979) 301–308.
[24] R.B. Bhat, Natural frequencies of rectangular plates using characteristic orthogonal polynomials in Rayleigh-Ritz method, J. Sound Vib. 102 (1985) 493–499.
[25] K.M. Liew, K.Y. Lam, A set of orthogonal plate functions for vibration analysis of regular polygonal plates, Trans. Amer. Soc. Mech. Engrs.: J. Vib. Acoust. 113 (1991) 182–186.
[26] C.W. Lim, K.M. Liew, Vibrations of perforated plates with rounded corners, J. Engrg. Mech. 121 (2) (1995) 203–213.

[27] K.M. Liew, C.M. Wang, Y. Xiang, S. Kitipornchai, Vibration of Mindlin Plates, Programming the p-Version Ritz Method, Elsevier, Amsterdam, 1998.

[28] A.Y.T. Leung, J.K.W. Chan, Fourier p-element for analysis of beams and plates, J. Sound Vib. 212 (1) (1998) 179–185.

[29] O.C. Zienkiewicz, R.L. Taylor, The Finite Element Method, vol. 1, New York, McGraw-Hill, 1989.

[30] N.S. Bardell, J.M. Dunsdon, R.S. Langley, Free vibration of coplanar sandwich panels, Compos. Struct. 38 (1997) 463–475.

[31] Y.K. Cheung, W.J. Chen, Hybrid quadrilateral element based on Mindlin/Reissner plate theory, Comput. Struct. 32 (1989) 327–339.

[32] R. Bellman, B.G. Kashef, J. Casti, Differential quadrature: a technique for the rapid solution of non-linear partial differential equations, J. Comput. Phys. 10 (1972) 40–52.

[33] C.W. Bert, S.K. Jang, A.G. Striz, Two new approximate methods for analyzing free vibration of structural components, Amer. Inst. Aeronaut. Astronaut. J. 26 (1988) 612–618.

[34] S.K. Jang, C.W. Bert, A.G. Striz, Application of differential quadrature to static analysis of structural components, Int. J. Numer. Methods Engrg. 28 (1989) 561–577.

[35] J.R. Quan, C.T. Chang, New insights in solving distributed system of equations by the quadrature method—I. Analysis, Comput. Chem. Engrg. 13 (1989) 779–788.

[36] W. Chen, T.X. Zhong, A note on the DQ analysis of anisotropic plates, J. Sound Vib. 204 (1) (1997) 180–182.

[37] C. Shu, B.E. Richards, Application of generalized differential quadrature to solve two–dimensional incompressible Navier–Stokes equations, Int. J. Numer. Methods Fluids 15 (1992) 791–798.

[38] H. Du, M.K. Lim, R.M. Lin, Application of generalized differential quadrature method to structure problems, Int. J. Numer. Methods Engrg. 37 (1994) 1881–1896.

[39] C. Shu, H. Du, A generalized approach for implementing general boundary conditions in the GDQ free vibration analysis of plates, Int. J. Solids Struct. 34 (1997) 837–846.

[40] C. Shu, C.M. Wang, Treatment of mixed and non-uniform boundary conditions in GDQ vibration analysis of rectangular plate, Engrg. Struct. 21 (1999) 125–134.

[41] G.W. Wei, Discrete singular convolution for the solution of the Fokker–Planck equation, J. Chem. Phys. 110 (1999) 8930–8942.

[42] G.W. Wei, A unified approach for the solution of the Fokker–Planck equation, J. Phys. A: Math. Gen. 33 (2000) 4935–4953.

[43] G.W. Wei, Wavelets generated by using discrete singular convolution kernels, J. Phys. A: Math. Gen. 33 (2000) 8577–8596.

[44] L. Schwarz, Théore des Distributions, Hermann, Paris, 1951.

[45] G.W. Wei, A new algorithm for solving some mechanical problems, Comput. Methods Appl. Mech. Engrg. 190 (2001) 2017–2030.

[46] D.C. Wan, B.S.V. Patnaik, G.W. Wei, Discrete singular convolution-finite subdomain method for the solution of incompressible viscous flows, J. Comput. Phys. 180 (2002) 229–255.

[47] G.W. Wei, Discrete singular convolution method for the sine-Gordon equation, Physica D 137 (2000) 247–259.

[48] S. Guan, C.-H. Lai, G.W. Wei, Fourier–Bessel analysis of patterns in a circular domain, Physica D 151 (2001) 83–98.

[49] G.W. Wei, Synchronization of single-side locally averaged adaptive coupling and its application to shock capturing, Phys. Rev. Lett. 86 (2001) 3542–3545.

[50] G.W. Wei, Generalized Perona–Malik equation for image restoration, IEEE Signal Process. Lett. 6 (1999) 165–168.

[51] G.W. Wei, Discrete singular convolution for beam analysis, Engrg. Struct. 23 (2001) 1045–1053.

[52] G.W. Wei, Vibration analysis by discrete singular convolution, J. Sound Vib. 244 (2001) 535–553.

[53] Y.B. Zhao, G.W. Wei, DSC analysis of rectangular plates with nonuniform boundary conditions, J. Sound Vib. 255 (2002) 203–225.

[54] G.W. Wei, Y.B. Zhao, Y. Xiang, Discrete singular convolution and its application to the analysis of plates with internal supports—I. Theory and algorithm, Int. J. Numer. Methods Engrg. 55 (2002) 913–946.

[55] Y.B. Zhao, G.W. Wei, Y. Xiang, Plate vibration under irregular internal supports, Int. J. Solids Struct. 39 (5) (2002) 1361–1383.

[56] Y.B. Zhao, G.W. Wei, Y. Xiang, Discrete singular convolution for the prediction of high frequency vibration of plates, Int. J. Solids Struct. 39 (1) (2002) 65–88.

[57] G.W. Wei, Y.B. Zhao, Y. Xiang, A novel approach for the analysis of high frequency vibrations, J. Sound Vib. 257 (2002) 207–246.